

Quantitative comparison of dynamic flux distribution of magnetic couplers for roadway electric vehicle wireless charging system

Chun Qiu, K. T. Chau, Chunhua Liu, Wenlong Li, and Fei Lin

Citation: [Journal of Applied Physics](#) **115**, 17A334 (2014); doi: 10.1063/1.4866882

View online: <http://dx.doi.org/10.1063/1.4866882>

View Table of Contents: <http://scitation.aip.org/content/aip/journal/jap/115/17?ver=pdfcov>

Published by the [AIP Publishing](#)

Articles you may be interested in

[Field weakening capability investigation of an axial flux permanent-magnet synchronous machine with radially sliding permanent magnets used for electric vehicles](#)

J. Appl. Phys. **111**, 07A719 (2012); 10.1063/1.3676230

[Permanent magnet online magnetization performance analysis of a flux mnemonic double salient motor using an improved hysteresis model](#)

J. Appl. Phys. **111**, 07D119 (2012); 10.1063/1.3676049

[Design and analysis of new fault-tolerant permanent magnet motors for four-wheel-driving electric vehicles](#)

J. Appl. Phys. **111**, 07E713 (2012); 10.1063/1.3672853

[A flux-mnemonic permanent magnet brushless motor for electric vehicles](#)

J. Appl. Phys. **103**, 07F103 (2008); 10.1063/1.2830553

[Use of a thermophotovoltaic generator in a hybrid electric vehicle](#)

AIP Conf. Proc. **460**, 488 (1999); 10.1063/1.57831



Quantitative comparison of dynamic flux distribution of magnetic couplers for roadway electric vehicle wireless charging system

Chun Qiu, K. T. Chau,^{a)} Chunhua Liu, Wenlong Li, and Fei Lin

Department of Electrical and Electronic Engineering, The University of Hong Kong Pokfulam Road, Hong Kong, China

(Presented 6 November 2013; received 23 September 2013; accepted 22 November 2013; published online 27 February 2014)

This paper gives a quantitative comparison of magnetic couplers for electric vehicle (EV) wireless charging applications. Circular pad with ferrite spokes and coreless rectangular coils are specially selected for analysis. The dynamic flux density between couplers under high misalignment is studied by calculating the uncompensated power of the pick-up coupler. By using finite element analysis, the performance of each type of coupler is evaluated, and its adaptation to on-road EV charging are compared according to the flux distribution and effective charging area. © 2014 AIP Publishing LLC. [<http://dx.doi.org/10.1063/1.4866882>]

I. INTRODUCTION

The development of electric vehicles (EVs) has been hindered by the costly battery and inconvenient battery recharging.¹ A roadway charging system employing wireless power transfer technology is anticipated to solve this problem. Two types of charging infrastructures are generally used, namely, the lumped magnetic couplers and straight line buried rail. The rail type is welcomed by the move-and-charge application for its evenly distributed magnetic field at each cross-section along the rail. However, its installation and arrangement are inflexible and costly. The lumped couplers offer better flexibility and lower cost, and are mainly used for stationary charging since the mutual inductance of couplers varies significantly with the vehicle position. Recently, some researches have been done on the misalignment adaption.²⁻⁴ With effective control strategies, the lumped magnetic couplers can support the desired constant power for move-and-charge application.

In this paper, two most common lumped couplers are evaluated on the perspective of on-road charging application: the circular pad with ferrite spokes and flat coreless rectangular coils. The uncompensated power of the pick-up coupler P_{UN} is chosen as a simple and intuitive way to evaluate the flux distribution and coupling performance. Then, two pairs of couplers with the same power supply, load rating, and dimension constraints are designed for comparison. Finite element analysis (FEA) is employed to directly evaluate the flux density distribution, and to calculate P_{UN} at different horizontal offsets of the couplers. Finally, the effective charging ranges of two types of couplers are compared with emphasis on the power fluctuation and leakage flux density. The rectangular couplers show a much wider charging range but with a slightly higher leakage flux as compared with the circular couplers.

II. ROADWAY WIRELESS CHARGING SYSTEM

Fig. 1 shows a typical schematic of the EV wireless charging system. The power is drawn from a single-phase or three-phase AC supply. The active front end rectifier is used to achieve unity power factor. The primary coil L_1 is fed by a current source converter operating at tens of kilohertz to several hundred kilohertz. The secondary coil L_2 which locates close to the primary coil should be able to capture sufficient amount of magnetic flux. For EV application, the gap between these two coils should be 150 mm to 200 mm to tolerate actual road conditions. Two capacitors C_1 and C_2 are connected in series with L_1 and L_2 , respectively, to form a resonant compensation network, hence maximizing the load power and lowering the volt-ampere (VA) rating of the power supply.⁵ The series-series topology is selected because the optimal operating frequency is independent of the magnetic coupling and load condition, which is especially convenient for the roadway application.

For magnetic couplers, the performance is related to both self-inductance and mutual inductance on both sides. It can be simply evaluated using the magnetic coupling coefficient k as given by

$$k = \frac{M}{\sqrt{L_1 L_2}}, \quad (1)$$

where M is the mutual inductance which is subject to the relative position of the couplers. The power transferred to the load P_L is defined as

$$P_L = \frac{M^2}{L_2} \omega I_p^2 Q = V_{OC} I_{SC} Q^{SC} = P_{UN} Q, \quad (2)$$

where ω is the operating frequency, I_p is the primary current, V_{OC} and I_{SC} are the open-circuit voltage and short-circuit current of the secondary coupler, and Q is the secondary quality factor which can be tuned by controlling the equivalent load impedance. While L_1 and L_2 are relatively constant at different horizontal offsets, especially with a large air gap,

^{a)}Electronic mail: ktchau@eee.hku.hk.

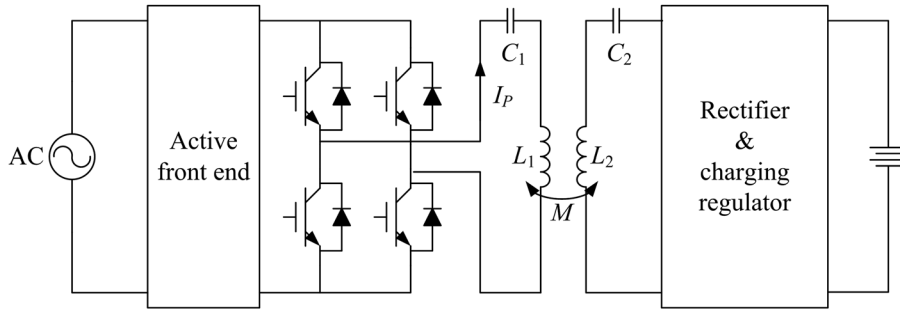


FIG. 1. Schematic of typical wireless power transfer system.

k has a square relationship with P_L . Thus, the mostly related and invariant parameter to k is P_{UN} which is the product of V_{OC} and I_{SC} , and it is easy to be measured. Therefore, P_{UN} is chosen as the index to evaluate the performance of the couplers.

In this paper, a roadway EV wireless charging system having the power of 2 kW and air gap of 200 mm is used for exemplification, which is suitable for most passenger EVs. Two types of magnetic couplers are designed based on the same power and performance demands, as shown in Figs. 2 and 3.

As the optimal air gap is close to 1/4 of the diameter,³ the diameter of the circular couplers is set to 700 mm. Ferrite spokes are used to guide the magnetic flux, thus enhancing the coupling performance. However, a large number of narrow spokes may reduce the mechanical strength. The selection of primary and secondary turn ratio should consider the load power, load voltage, supply current, and operating frequency. Since the purpose of this paper is to evaluate the performance of couplers, the turn ratio is simply selected as 1:1.

The design of rectangular couplers is simple. Each coupler has a square coil with the outside length of 700 mm, which is essentially the same size as the circular coupler. Detailed specifications of both couplers are shown in Table I.

III. COMPARISON AND RESULTS

To evaluate the dynamic flux distribution of the two types of couplers, a three-dimensional FEA tool JMAG is adopted. The simulation is carried out at different horizontal offsets

between the primary and secondary couplers. Namely, P_{UN} is evaluated at each position by separately calculating V_{OC} and I_{SC} of the secondary coupler.

Fig. 4 shows the characteristics of P_{UN} versus different horizontal offsets with an air gap of 200 mm. It can be observed that the rectangular coupler shows better performance in both power rating and misalignment tolerance. It is noteworthy that the circular coupler begins to offer insignificant P_{UN} when the horizontal offset is larger than 300 mm, indicating that the load will not receive any power regardless of the regulation. Since the radius of the coupler is larger than 300 mm, there will be an absence of power on the load even all primary couplers are put

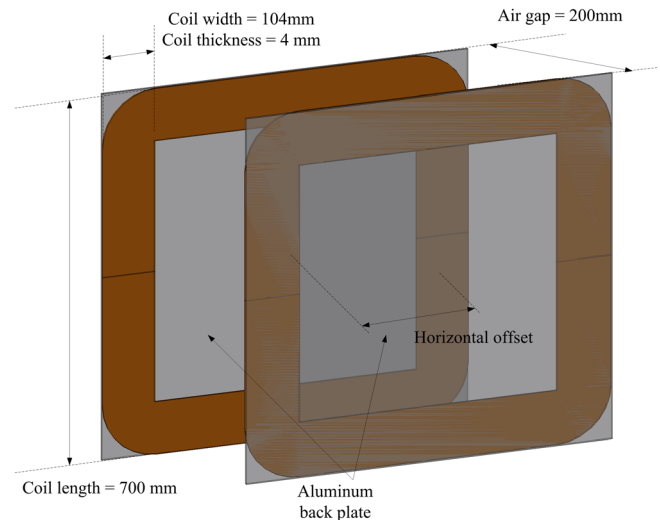


FIG. 3. Layout of 700 mm rectangular couplers.

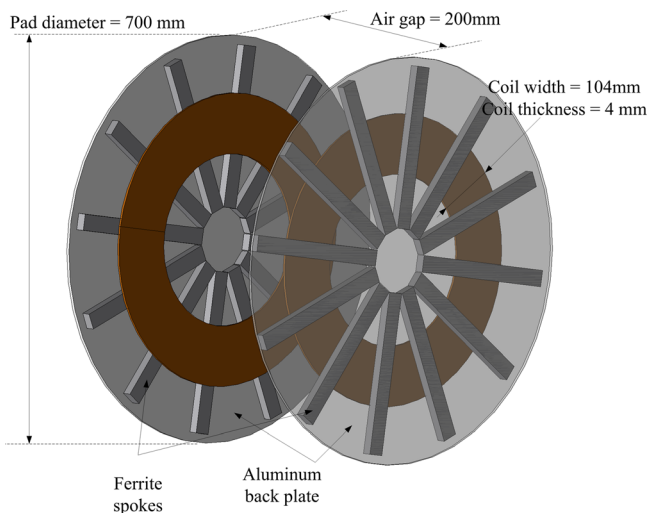


FIG. 2. Layout of 700 mm circular couplers with ferrite spokes.

TABLE I. Design specifications.

	Circular couplers	Rectangular couplers
No. of primary coil turns	26	25
No. of secondary coil turns	26	25
Coil thickness	4 mm	4 mm
Air gap	200 mm	200 mm
Primary current	23 A	23 A
Operating frequency	20 kHz	20 kHz
Ferrite width	28 mm	...
Ferrite length	279 mm	...
Ferrite thickness	16 mm	...
Aluminum plate width	700 mm	700 mm
Aluminum plate thickness	5 mm	5 mm
Coil central diameter	400 mm	...
Coil length	...	700 mm

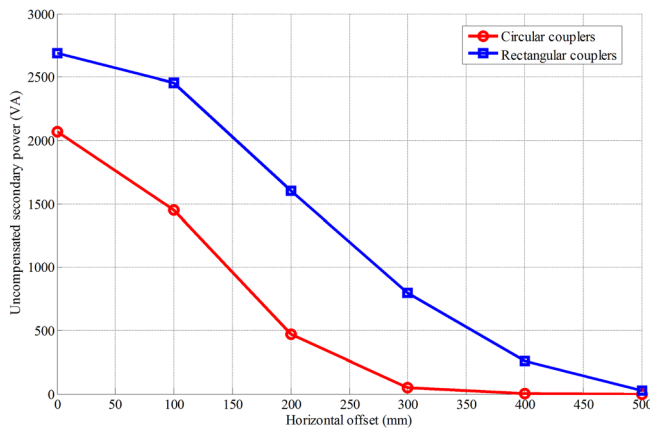


FIG. 4. Characteristics of uncompensated secondary power versus horizontal offset with 200 mm air gap.

close to each other. Moreover, unlike the rectangular couplers, there are inevitable holes between the circular pads. This will further increase the zero power zones. Consequently, if adopting the circular couplers, the multilayer arrangement will be required to achieve the desired power transfer. For the rectangular coupler, the power does not die out until the offset reaches 500 mm. The secondary quality factor is normally from 4 to 6, which is governed by the electrical stress of circuit components. Thus, the load power can reach the rated value of 2 kW even with a horizontal offset of 350 mm ($Q=4$). So if the adjacent couplers are close to each other, the power will be constant along the road.

As the unwanted leakage flux may bring up safety issues, the International Commission on Non-Ionizing Radiation Protection (ICNIRP) suggests that the acceptable human exposure to electromagnetic field should be less than $6.25 \mu\text{T}$ at frequency 0.8–150 kHz.⁶ When the couplers are at the horizontal offset of 200 mm and the load power is 2 kW, the leakage flux densities at different locations are calculated by using FEA. As shown in Fig. 5, within the horizontal and vertical displacements of 1500 mm, the leakage flux densities of both circular and rectangular couplers are mostly greater than the threshold of $6.25 \mu\text{T}$. This is anticipated as there is no shielding adopted in this analysis, and it can readily be improved by adding shielding rings⁴ or reactive loops.⁷ Meanwhile, it can be observed that although the rectangular coupler can offer good performance on misalignment tolerance, its leakage flux is generally larger than that of the circular coupler, especially at the location with vertical displacement, which is a concern for EV users.

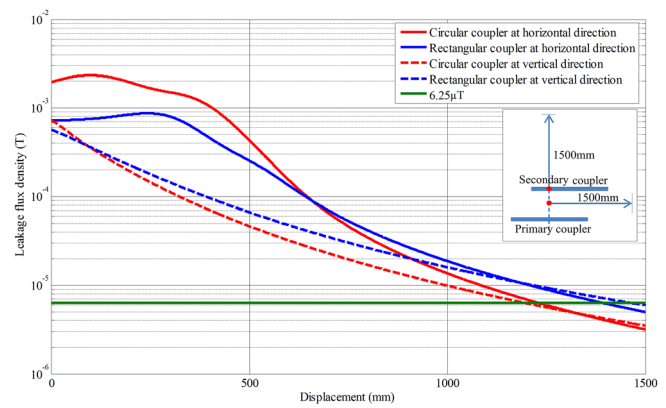


FIG. 5. Leakage flux density analysis at 200 mm horizontal offset.

IV. CONCLUSION

This paper evaluates and compares two different types of magnetic couplers for EV move-and-charge application. Two sets of couplers are designed for a 2 kW system with an air gap of 200 mm. The uncompensated secondary power is selected as the index for performance evaluation. The characteristics at different offsets and the magnetic field distributions are simulated by using finite element analysis. The results show that the coreless rectangular coupler can offer better performance than the commonly adopted circular coupler with ferrite spokes for EV charging application, though it exhibits higher leakage flux in the absence of shielding.

ACKNOWLEDGMENTS

This work was supported by a Grant (Project No. HKU SPF 201109176034) from the Committee on Research and Conference Grants, The University of Hong Kong, Hong Kong.

¹C. C. Chan and K. T. Chau, *Modern Electric Vehicle Technology* (Oxford University Press, 2001).

²T. Misawa, T. Sato, T. Takura, F. Sato, and H. Matsuki, *J. Appl. Phys.* **111**, 07E720 (2012).

³M. Budhia, G. A. Covic, and J. T. Boys, *IEEE Trans. Power Electron.* **26**, 3096 (2011).

⁴J. Sallan, J. L. Villa, A. Llombart, and J. F. Sanz, *IEEE Trans. Ind. Electron.* **56**, 2140 (2009).

⁵G. A. Covic and J. T. Boys, *Proc. IEEE*, **101**, 1276 (2013).

⁶ICNIRP Guidelines, *Health Phys.* **74**, 494 (1998).

⁷J. Kim, J. Kim, S. Kong, H. Kim, I. S. Suh, N. P. Suh, D. H. Cho, J. Kim, and S. Ahn, *Proc. IEEE*, **101**, 1332 (2013).